

SAMPLING DELAY AND BACKLASH IN BALANCING SYSTEMS

László E. KOLLÁR*, Gábor STÉPÁN* and S. John HOGAN**

* Department of Applied Mechanics
Technical University of Budapest
H-1521 Budapest, Hungary
e-mail: lakol@mm.bme.hu

** Department of Engineering Mathematics
University of Bristol
Bristol BS8 1TR, UK

Received: Sept. 5, 1999

Abstract

A mechanical model of a digital balancing system is constructed and its stability analysis is presented. This model considers experimental problems like backlash and sampling delay. The conditions of existence of stable stationary and periodic solutions are determined for the case of the system without delay. Phase diagrams and bifurcation diagrams are revealed after simulations and bifurcation analysis. Adding sampling delay to the system, the stability conditions are changed and above a critical value of the delay, the balancing is impossible. The stability conditions and the stability chart are determined again and the critical sampling delay is calculated versus the parameters describing the system.

Keywords: sampling delay, backlash, bifurcation analysis.

1. Introduction

Unstable equilibria of mechanical systems often have to be stabilized by control force. A number of applications can be found in this field, e.g. the bus running on icy road, the shimmying wheel or the balancing of standing and walking robots. A lot of problems occur during stabilization. Time delay, driving through elastic belt or backlash at the driving-wheel of the motor tend to destabilize dynamical systems.

A typical example of stabilization of unstable equilibria is the balancing. The simplest model of balancing is that of the inverted pendulum [1,2,3,4,5]. The angle and the angular velocity of the pendulum are detected and a horizontal control force at the lowest point of the pendulum is determined by them in a way that the stick should be balanced at its upper position. Control parameters must be chosen from a bounded region for successful balancing. The stability conditions have been calculated and the stability chart in the plane of the control parameters has been constructed in earlier works [6]. The stability domain shrinks as the time delay increases and above a critical value of the delay, the successful balancing of the upper position of the pendulum is impossible.

A digital balancing system is considered in the subsequent chapters. The inverted pendulum and the motor displaying the control force are placed on a cart and the motor drives one of the wheels of the cart through a teeth-belt. Controlling is executed by a computer which is situated outside this cart. There are two general factors which influence the stability conditions: sampling delay and stiffness of the driving-belt. Increasing time delay or elasticity of the driving-belt tends to destabilize the examined system. Considering the backlash at the driving-wheel of the motor, the pendulum will swing with small amplitude around its equilibrium. The stability domain in the plane of the control parameters does not change, but an unstable zone appears in the phase diagram.

2. The Mechanical Model and the Stability Analysis

In order to describe a digital balancing system, the inverted pendulum is placed on a cart as it can be seen in *Fig. 1* [7,8]. The motor drives one of the wheels of this cart through a teeth-belt with stiffness s . The system has 3 degrees of freedom described by the general coordinates, x , φ and ψ . The angle φ of the pendulum and the displacement x of the cart are detected together with their derivatives.

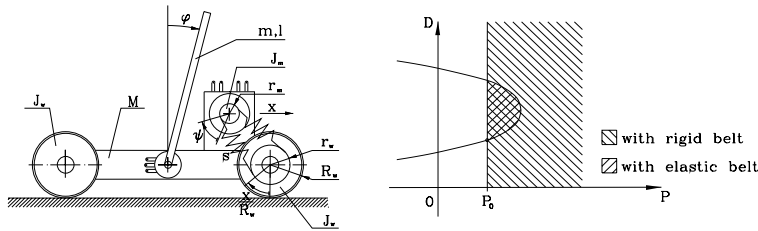


Fig. 1. The inverted pendulum on a cart and its stability map

The control force is determined by the motor characteristic. The driving-torque is linearly proportional to the voltage U_m of the motor and to the angular velocity $\dot{\psi}$:

$$M_m = LU_m - K\dot{\psi}. \quad (1)$$

Considering PD controllers, we have:

$$U_m = P\varphi + D\dot{\varphi} + P_x x + D_x \dot{x}. \quad (2)$$

The system can be stabilized if the displacement of the cart is not detected ($P_x = 0$) and the differential gain D_x of the cart eliminates the damping K of the motor. Then the control force has this simplified form:

$$Q = L(P\varphi + D\dot{\varphi}). \quad (3)$$

The system is reduced to a system with 2 degrees of freedom if a new general coordinate is introduced. This is Δ , the elongation of the spring:

$$\Delta = r_m \psi - \frac{r_w}{R_w} x. \quad (4)$$

The linearized equations of motion assume the form:

$$\begin{pmatrix} \frac{(m+M)m_m r_m}{2} & -\frac{m m_m l r_m r_w}{4 R_w} \\ 0 & \frac{m l^2}{3} - \frac{m^2 l^2}{4(m+M)} \end{pmatrix} \begin{pmatrix} \ddot{\Delta} \\ \ddot{\varphi} \end{pmatrix} + \begin{pmatrix} (m+M) \frac{K}{r_m} & 0 \\ 0 & 0 \end{pmatrix} \begin{pmatrix} \dot{\Delta} \\ \dot{\varphi} \end{pmatrix} + \begin{pmatrix} 0 & 0 \\ 0 & -\frac{m g l}{2} \end{pmatrix} \begin{pmatrix} \Delta \\ \varphi \end{pmatrix} + \begin{pmatrix} (m+M) r_m + \frac{m_m r_m r_w^2}{2 R_w^2} \\ \frac{m l r_w}{2(m+M) R_w} \end{pmatrix} R_s = \begin{pmatrix} (m+M) Q \\ 0 \end{pmatrix}, \quad (5)$$

where

$$R_s = \begin{pmatrix} -s \frac{r_w}{R_w} & 0 & s r_m \end{pmatrix} \begin{pmatrix} x \\ \varphi \\ \psi \end{pmatrix} = s \Delta \quad (6)$$

is the force in the spring.

The stability analysis is carried out by the Routh–Hurwitz criterion. If the belt is ideally rigid, then $\Delta = 0$, x determines ψ uniquely, so the system has 2 degrees of freedom, namely x and φ . The $\varphi \equiv 0$ trivial solution of this system is asymptotically stable if and only if

$$P > P_0 = \frac{1}{L} \left[\left(m + M + \frac{1}{2} m_m \frac{r_w^2}{R_w^2} \right) g \frac{r_m R_w}{r_w} \right] \quad \text{and} \quad D > 0. \quad (7)$$

If the belt is elastic, then the trivial solution of (4) is asymptotically stable if and only if

$$P > P_0 \quad \text{and} \quad H_2 > 0, \quad (8)$$

where H_2 is the maximum sized Hurwitz determinant, not presented here algebraically.

The stability chart is constructed as it is shown in *Fig. 1*. The stability domain shrinks as the stiffness of the driving-belt decreases and at a certain critical value, it disappears. This critical value has this form:

$$s > s_{\text{crit}} = \frac{3(m+M)m_m g}{\left(m + 4M + 2m_m \frac{r_w^2}{R_w^2}\right) l}. \quad (9)$$

3. Numerical Study of the Phase-Space

Backlash appears in the system as a nonlinear spring characteristic. The force in the spring is the function of Δ :

$$R_s = \begin{cases} s (\Delta + r_0) & \Delta \leq -r_0 \\ 0 & |\Delta| < r_0 \\ s (\Delta - r_0) & \Delta \geq r_0 \end{cases}, \quad (10)$$

where r_0 is the value of backlash. This function is given in *Fig. 2*.

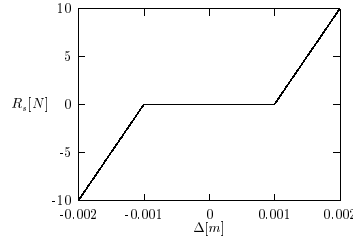


Fig. 2. The nonlinear spring characteristic at $s = 10[\frac{\text{kN}}{\text{m}}]$ and $r_0 = 1[\text{mm}]$

New constant expressions appear in the equations of motion, that means shifting of the solutions. The stability domain does not change but it is valid only if $|\Delta| > r_0$. Otherwise, the system is just in backlash, so it cannot be stabilized, because the control force is not displayed in this little domain.

If the control parameters are chosen from the stability domain, then roots of the characteristic equation are complex numbers with negative real parts. Trajectories form stable focus around the $(\varphi, \dot{\varphi}, \Delta, \dot{\Delta}) = (0, 0, \pm r_0, 0)$ equilibria.

If the system is just in backlash, then the roots of the characteristic equation are positive and negative reals. Trajectories form saddle around the $(0, 0, 0, 0)$ equilibrium.

Simulations were accomplished for the study of the phase-space [9]. Results are presented in *Fig. 3(a)* and *3(b)* near different values of either of the control parameters, P . The $(0, 0, \pm r_0, 0)$ equilibria are stable for smaller values of P . A stable periodic solution appears for greater values of P and its amplitude is larger and larger as P increases. Its amplitude tends to infinity as P tends to the border of the stability domain. Now the stability domain means the domain where stable stationary or periodic solution can be found. The physical meaning of the periodic solution is the oscillation of the stick around its vertical equilibrium. The physical meaning of the stable fix points is that the control force does not push the stick further than the vertical line and it oscillates with less and less amplitude on either side of the vertical position. For certain values of P all the $(0, 0, \pm r_0, 0)$ equilibria

and the limit cycle are stable and trajectories spiral to one of them depending on the initial conditions. More investigations are needed for the exact knowledge of the phase-space.

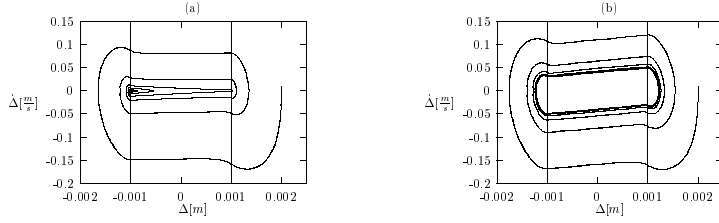


Fig. 3. Phase diagram on $\dot{\Delta} - \Delta$ plane, (a) $P = 2, D = 2$, (b) $P = 20, D = 2$

4. The Bifurcation Analysis

The bifurcation diagram was also examined numerically. The spring characteristic has a noncontinuous first derivative and this caused problems during determining periodic solutions. Therefore two approximate spring characteristics were applied as they are shown in Fig. 4. Both of them include a parameter K_s , and approximations are more and more accurate, as it tends to infinity.

$$R_{s1} = \frac{s}{K_s} \ln \frac{1 + e^{K_s(\Delta - r_0)}}{1 + e^{-K_s(\Delta + r_0)}},$$

$$R_{s2} = \begin{cases} s(\Delta + r_0) & \Delta \leq -r_0 \\ s(\Delta - r_0)e^{K_s(\Delta - r_0)} + s(\Delta + r_0)e^{-K_s(\Delta + r_0)} & |\Delta| < r_0 \\ s(\Delta - r_0) & \Delta \geq r_0 \end{cases} \quad (11)$$

A stable periodic solution can be obtained with both of the approximations. These solutions are closer and closer to each other as K_s increases. The limit between the two kinds of approximation is the solution with respect to the exact piecewise linear system. The periodic solution appears at certain pairs of P, D values. Approaching one of these pairs, the period of the solution increases as it can be seen in Fig. 5(a), and a homoclinic orbit shows up for these pairs as it is shown in Fig. 5(b).

The bifurcation diagrams are presented in Fig. 6(a) and 6(b), where the bifurcation parameters are the control parameters, P and D . $D = 2$ in Fig. 6(a). There is a branch point at either border of the stability domain where stable fix points appear. A homoclinic orbit occurs at a certain value of P , so there is a homoclinic

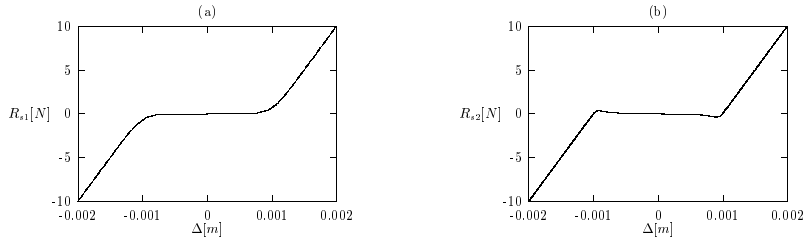


Fig. 4. Approximate spring characteristics at $s = 10[\frac{\text{kN}}{\text{m}}]$, $r_0 = 1[\text{mm}]$ and $K_s = 10^4$
 (a) R_{s1} , (b) R_{s2}

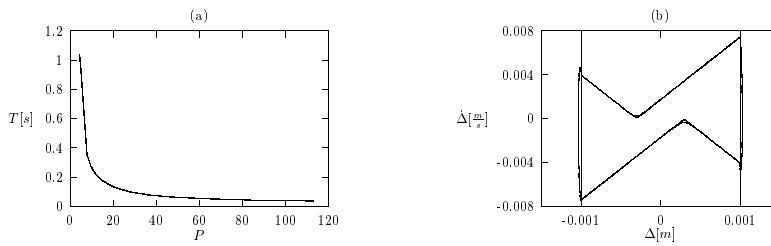


Fig. 5. (a) Period of the periodic solution at $D = 2$, (b) The homoclinic orbit at $P = 3.46$ and $D = 2$

bifurcation there, where a limit cycle appears. All the fix points and the limit cycle are stable in a domain for greater values of P . All of them have a domain of attraction, so trajectories spiral to one of them depending on the initial conditions. There is another bifurcation point at another value of P , where the fix points become unstable. The periodic solution retains its stability till the parameters reach the other border of the stability domain with increasing amplitude.

$P = 50$ in Fig. 6(b). There is a stable limit cycle between the borders of the stability domain but the fix points are stable only along the continuous line between the bifurcation points indicated with squares in the figure.

After the bifurcation analysis the stability chart in the plane of the control parameters can be constructed as it can be seen in Fig. 7(a). It is bordered with the same straight line and parabola as it was bordered in case of the linear system (the system without backlash). Fix points are stable in a little domain near the straight line. Stable limit cycle appears at the homoclinic bifurcation point indicated with the dotted line. Fix points lose their stability at the other bifurcation point indicated with the smashed line, so all the fix points and the limit cycle are stable between

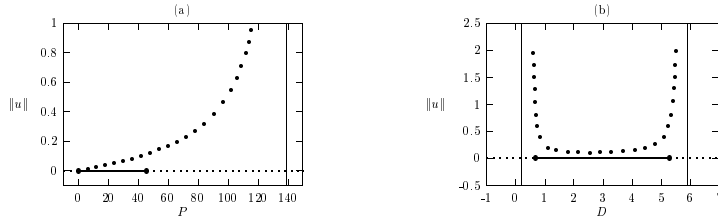


Fig. 6. Bifurcation diagrams, the bifurcation parameter is (a) P , (b) D

the dotted and the smashed line, and only the limit cycle is stable in the remaining part of the stability domain.

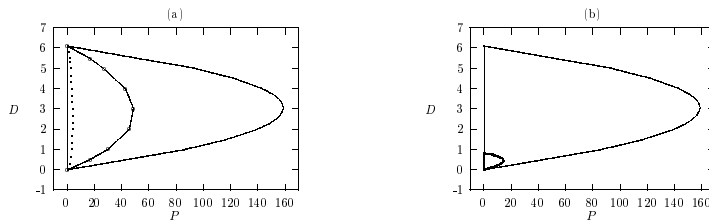


Fig. 7. (a) The stability chart with the bifurcation curves, (b) The stability charts without and with sampling delay

5. Backlash and Sampling Delay Together

Regarding the sampling delay τ the system becomes discrete. Simulations and investigation of the phase-space are implemented again. The character of the stability domain is the same as it was at the system without time delay, but it is smaller and smaller as the time delay increases. The stability chart is given in Fig. 7(b) for $\tau = 0[s]$ and $\tau = 0.005[s]$.

Balancing of the pendulum is impossible above a critical value of the sampling delay as it was mentioned earlier. This critical value depends on the parameters describing the system. The connection between the critical sampling delay and the length of the pendulum is shown in Fig. 8(a) and between the critical sampling delay and the spring stiffness is shown in Fig. 8(b). An asymptote can be seen in this figure, which is the same as the result of the examination of the system with rigid belt.

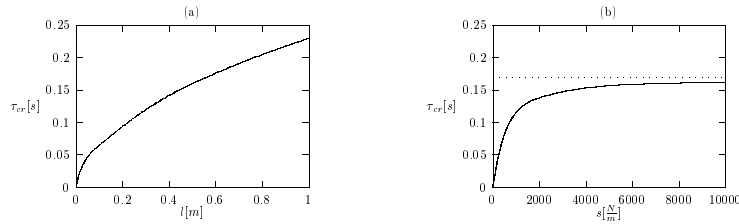


Fig. 8. (a) The critical sampling delay vs. the length of the pendulum, (b) The critical sampling delay vs. the spring stiffness

6. Conclusions

Increasing time delay and decreasing spring stiffness of the driving belt tend to destabilize the digitally controlled dynamical systems. Backlash causes oscillations of the pendulum around its upper equilibrium. It behaves as a spatial delay. The examined model is an example for the problems of stabilization of unstable equilibria of mechanical systems, but the main principles and methods are valid for stabilization of unstable equilibria of any other controlled mechanical systems.

Acknowledgement

This research was supported by the Hungarian Scientific Research Foundation under grant no. OTKA T030762 and the Ministry of Culture and Education under grant no. FKFP 0380/97.

References

- [1] HIGDON, D. T. – CANNON, R. H.: On the Control of Unstable Multiple-output Mechanical Systems, *ASME Publications*, Vol. 63-WA-48, (1963) pp. 1–12.
- [2] MORI, S. – NISHIHARA, H. – FURUTA, K.: Control of an Unstable Mechanical System, *Int. J. Control*, Vol. 23, (1976) pp. 673–692.
- [3] STÉPÁN, G.: A Model of Balancing, *Periodica Polytechnica*, Vol. 28, (1984) pp. 195–199.
- [4] HENDERS, M. G. – SONDAK, A. C.: ‘In-the-large’ Behaviour of an Inverted Pendulum with Linear Stabilization, *Int. J. of Nonlinear Mechanics*, Vol. 27, (1992) pp. 129–138.
- [5] KAWAZOE, Y.: Manual Control and Computer Control of an Inverted Pendulum on a Cart, *Proc. 1st Int. Conf. on Motion and Vibration Control*, pp. 930–935, Yokohama, 1992.
- [6] STÉPÁN, G. – KOLLÁR, L. E.: Balancing with Reflex Delay, *Mathematical and Computer Modelling*, accepted in 1997.
- [7] ENIKOV, E. – STÉPÁN, G.: Micro-Chaotic Motion of Digitally Controlled Machines, *J. of Vibration and Control*, accepted in 1997.
- [8] KOLLÁR, L. E.: Backlash in Machines Stabilized by Control Force, *Proc. of First Conference on Mechanical Engineering*, pp. 147–151, Budapest, 1998.
- [9] LÓRÁNT, G. – STÉPÁN, G.: The Role of Non-Linearities in the Dynamics of a Single Railway Wheelset, *Machine Vibration*, Vol. 5, (1996) pp. 18–26.